

Total arrest of spontaneous and evoked synaptic transmission but normal synaptogenesis in the absence of Munc13-mediated vesicle priming

Frederique Varoqueaux^{*†}, Albrecht Sigler^{*†}, Jeong-Seop Rhee^{*†}, Nils Brose^{*†}, Carsten Enk^{*}, Kerstin Reim^{*§}, and Christian Rosenmund^{*§}

^{*}Max-Planck-Institute for Experimental Medicine, Department of Molecular Neurobiology, D-37075 Göttingen, Germany; and [†]Max-Planck-Institute for Biophysical Chemistry, Department of Membrane Biophysics, D-37077 Göttingen, Germany

Edited by Erwin Neher, Max-Planck-Institute for Biophysical Chemistry, Göttingen, Germany, and approved April 18, 2002 (received for review November 23, 2001)

Synaptic vesicles must be primed to fusion competence before they can fuse with the plasma membrane in response to increased intracellular Ca^{2+} levels. The presynaptic active zone protein Munc13-1 is essential for priming of glutamatergic synaptic vesicles in hippocampal neurons. However, a small subpopulation of synapses in any given glutamatergic nerve cell as well as all γ -aminobutyrate (GABAergic) synapses are largely independent of Munc13-1. We show here that Munc13-2, the only Munc13 isoform coexpressed with Munc13-1 in hippocampus, is responsible for vesicle priming in Munc13-1 independent hippocampal synapses. Neurons lacking both Munc13-1 and Munc13-2 show neither evoked nor spontaneous release events, yet form normal numbers of synapses with typical ultrastructural features. Thus, the two Munc13 isoforms are completely redundant in GABAergic cells whereas glutamatergic neurons form two types of synapses, one of which is solely Munc13-1 dependent and lacks Munc13-2 whereas the other type employs Munc13-2 as priming factor. We conclude that Munc13-mediated vesicle priming is not a transmitter specific phenomenon but rather a general and essential feature of multiple fast neurotransmitter systems, and that synaptogenesis during development is not dependent on synaptic secretory activity.

Neurotransmitter release from neurons is restricted to synaptic active zones where the final steps of synaptic vesicle exocytosis take place in a highly coordinated manner. Typically, only a fraction of vesicles in close proximity of the active zone plasma membrane is primed (fusion competent) and able to fuse with the plasma membrane in response to an action potential and concomitant Ca^{2+} influx. The size of this readily releasable vesicle pool and its dynamic regulation by the priming machinery determine the efficacy and signaling capacity of synapses (1, 2).

The mammalian Unc-13 homologue Munc13-1 is an essential component of the synaptic vesicle priming machinery (3). Glutamatergic, hippocampal Munc13-1 knockout (KO) neurons form morphologically normal synapses, most of which are incapable of neurotransmission because their synaptic vesicles are not fusion competent (3). Similar observations were made in *Caenorhabditis elegans* and *Drosophila* lacking the invertebrate Munc13-1 homologues Unc-13 or Dunc-13 (4, 5). Interestingly, the mutant phenotype of Munc13-1 KO synapses in mouse hippocampus is restricted to glutamatergic neurons. γ -Aminobutyrate (GABAergic) cells are almost completely unaffected (3, 6). Moreover, individual glutamatergic hippocampal neurons form two types of synapses with differential Munc13-1 dependence where 90% of synapses are completely silenced in the absence of Munc13-1 whereas the remaining synapses release transmitter with normal probability (3, 6).

In contrast to the mouse protein, Munc13-1 homologues in *C. elegans* and *Drosophila* show no transmitter or synapse specific functions (4, 5). Although the genomes of these invertebrates contain only one *unc-13/dunc-13* gene each, the mammalian

Munc13 family is comprised of three independent gene products (Munc13-1, -2, and -3; refs. 7 and 8). Thus, the striking transmitter and synapse specificity of Munc13-1 function in mouse hippocampus may be caused by a redundancy with a second Munc13 isoform that can substitute for Munc13-1 in all GABAergic and a small subpopulation of glutamatergic synapses. Alternatively, neurons that are not affected by Munc13-1 loss may employ a Munc13-independent vesicle-priming mechanism.

To examine the role of other Munc13 isoforms in hippocampal neurons, we generated KO mice lacking both splice variants of Munc13-2 (9), the only known Munc13 isoform that is coexpressed with Munc13-1 in rodent hippocampus (8, 10).

Materials and Methods

Stem Cell Experiments. Munc13-2 KO mice were generated by homologous recombination in embryonic stem cells (3, 11, 12). In the targeting vector (Fig. 1A), a 6-kb genomic fragment containing multiple exons of the *Munc13-2* gene that are shared by the two Munc13-2 splice variants [bp 2907–3904 of bMunc13-2 cDNA (GenBank U24071); bp 1439–2436 of ub-Munc13-2 cDNA (GenBank AF159706)] was replaced by a neomycin resistance cassette. Recombinant stem cell clones were analyzed by Southern blotting of genomic DNA digested with *EcoRI*. Two of a total of three positive clones were injected into mouse blastocysts to obtain highly chimeric mice that transmitted the mutation through the germ line. Germ line transmission of the mutations was confirmed by Southern blotting (*EcoRI*; Fig. 1B). Immunoblotting of adult brain homogenates with an antibody recognizing both Munc13-2 splice variants demonstrated the total absence of Munc13-2 in mutant brains (Fig. 1C). Munc13-1/2 double KO mice (DKO) were generated by breeding and genotyped by Southern blotting, PCR, and Western blotting (Fig. 1D).

Cell Culture, Electrophysiology, Synapse Quantification, and FM1-43 Staining

Electrophysiological experiments were performed on individual autaptic hippocampal neurons [8–15 days *in vitro* (DIV)] from wild-type and Munc13-2 KO or Munc13-2 KO and Munc13-1/2 DKO littermates (13, 14). Data are expressed as mean \pm SE. Significance was tested by using Student's *t* test or one-way ANOVA with the Bonferroni-Dunn procedure for multiple comparisons (INSTAT; GraphPad Software, San Diego, CA). Semliki Forest virus experiments were performed as

This paper was submitted directly (Track II) to the PNAS office.

Abbreviations: KO, knockout; DKO, double knockout; GABAergic, γ -aminobutyrate; DIV, days *in vitro*; E18, embryonic day 18; mEPSC, miniature excitatory postsynaptic current; mIPSC, miniature inhibitory postsynaptic currents; MAP-2, microtubule-associated protein-2.

[†]F.V., A.S., J.-S.R., and N.B. contributed equally to this work.

[§]To whom reprint requests should be addressed. E-mail: reim@em.mpg.de or crosen@gwdg.de.

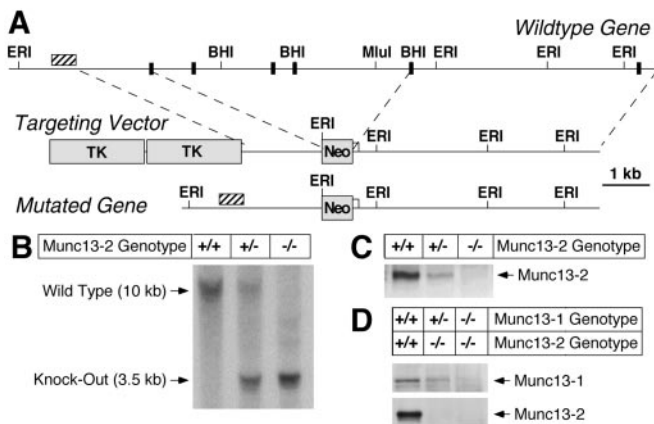


Fig. 1. Mutation of the murine *Munc13-2* gene. (A) Maps of the wild-type *Munc13-2* gene, the respective targeting vector, and the resulting mutant gene. Positions of exons (black boxes) and restriction enzyme sites are indicated. Hatched bar, Position of probe used for Southern. Neo, Neomycin resistance gene; TK, thymidine kinase gene. (B) Southern blot analysis of the *Munc13-2* KO mutations in mice by using mouse tail DNA (*EcoRI* digest) from the indicated *Munc13-2* genotypes. (C) *Munc13-2* protein expression in mice of the indicated genotypes as determined by Western blotting using an antibody that recognizes all *Munc13-2* splice variants. (D) Expression of *Munc13-1* and *Munc13-2* protein in mice of the indicated genotypes as determined by Western blotting using an antibody to *Munc13-1* (Upper) and an antibody that recognizes all *Munc13-2* splice variants (Lower).

described (9). For quantification of synapse density, neurons were fixed and double labeled for synaptophysin and microtubule-associated protein (MAP)-2. Fluorescence images were recorded as described (6). Pixel noise in the images was reduced by a “sharpening” function, followed by low pass filtering. Synapses were distinguished from background fluorescence by setting a threshold that shows only objects above this threshold intensity. Objects smaller than $0.17 \mu\text{m}^2$ were discarded; larger objects were detected by an object recognition algorithm and sorted by size. The average sized synapse was identified as the object that appeared at the highest frequency in the image. The proper threshold was calculated by a custom written algorithm that analyzed an image series with varying thresholds. Optimal threshold was determined when the total fluorescence intensity from the objects with highest occurrence ($0.53 \pm 0.14 \mu\text{m}^2$, 19 images, 20.622 objects) was maximal. Objects were considered to be synapses when their size was larger than 50% of the average synapse size. Spots whose summed fluorescence intensity was larger than twice the average were counted as two synapses. Data were expressed as synapse number per μm^2 dendrite surface. FM1-43 staining of active synapses was done as described (6).

Western Blotting, Histology, Electron Microscopy, and Antibodies. Synaptic protein expression in embryonic day 18 (E18) or adult brains was analyzed by Western blotting. For histological analyses, E18 mouse pups were immersion fixed in paraformaldehyde. Spinal cord and brain were then cryoprotected and frozen. Sagittal brain sections and coronal spinal cord sections ($10 \mu\text{m}$) were collected and Nissl stained. For electron microscopic analyses, primary hippocampal cultures were processed according to standard procedures. In brief, cultures (12 DIV) were fixed with glutaraldehyde and embedded in Durcupan. Ultrathin sections (55 nm) were observed in a Philips (Eindhoven, The Netherlands) CM 120 electron microscope. Digital pictures from synapses were taken and analyzed by using DIGITAL MICROGRAPH (Gatan, Pleasanton, CA). Vesicles within 6 nm of the active zone plasma membrane were defined as docked. The length of the active zone was defined as the length of presynaptic

membrane facing a postsynaptic specialization. Data are expressed as mean \pm SE. Significance was tested by using Student's *t* test and unpaired nonparametric test (Wilcoxon). All antibodies were from Synaptic Systems (Göttingen, Germany), except antibodies to *Munc13-2*, *Munc13-3*, MAP-2 (Chemicon), glutamic acid decarboxylase (GAD; Biotrend, Cologne, Germany), and Rab-3-interacting molecule (RIM) (Transduction Laboratories, Lexington, KY).

Results

Basic Characteristics of *Munc13-2* KO Mice. *Munc13-2* KO mice were generated as described above (Fig. 1A). Southern blot analysis of offspring obtained by interbreeding heterozygous *Munc13-2* KOs showed that the respective genotypes (+/+, +/-, and -/-) were present at the expected Mendelian frequency (Fig. 1B). *Munc13-2* protein expression was completely abolished in homozygous mutants and reduced by about 50% in heterozygous littermates (Fig. 1C). Apart from sporadic seizures in older animals (above 12 mo of age), *Munc13-2* KOs were indistinguishable from wild-type littermates. Brains of *Munc13-2* KOs showed a normal cell density, cytoarchitecture, connectivity, distribution/density of synapses, and ultrastructural morphology (not shown). Levels of all tested synaptic proteins (*Munc13-1*, soluble NSF-attachment protein (α -SNAP), complexin I, complexin II, *Munc18-1*, *N*-ethylmaleimide-sensitive factor (SNF), Rab3A, synaptosome-associated protein of 25 kDa (SNAP-25), synapsin I/IIa, synapsin IIb, synaptobrevin 2, synaptophysin, synaptotagmin I, and syntaxin 1) were unaffected by the lack of *Munc13-2* (not shown).

Properties of *Munc13-2* KO and *Munc13-1/2* DKO Neurons. Excitatory postsynaptic currents (EPSCs) from wild-type and *Munc13-2* KO neurons were not significantly different. EPSCs were $5.0 \pm 0.8 \text{ nA}$ ($n = 10$) for wild-type cells and $5.2 \pm 0.8 \text{ nA}$ ($n = 19$) for *Munc13-2* KO cells (Fig. 2A and B). Likewise, elimination of *Munc13-2* had no apparent effect on inhibitory synaptic transmission. IPSCs were $3.5 \pm 0.9 \text{ nA}$ ($n = 13$) for wild-type cells and $3.5 \pm 0.8 \text{ nA}$ ($n = 5$) for *Munc13-2* KO cells (Fig. 2E and F). Spontaneous miniature EPSC (mEPSC) frequencies/amplitudes and miniature inhibitory postsynaptic currents (mIPSC) frequencies/amplitudes were also not affected by the *Munc13-2* deletion (see examples in Fig. 2D and G). mEPSC frequencies/amplitudes were $3.2 \pm 0.9 \text{ Hz}/22.7 \pm 2.4 \text{ pA}$ ($n = 17$) in *Munc13-2* KO cells and $3.8 \pm 0.7 \text{ Hz}/22.0 \pm 1.9 \text{ pA}$ ($n = 23$) in wild-type cells. mIPSC frequencies/amplitudes were $2.8 \pm 0.9 \text{ Hz}/46 \pm 6 \text{ pA}$ ($n = 4$) in *Munc13-2* KO cells and $2.1 \pm 0.4 \text{ Hz}/43.4 \pm 4.5$ ($n = 13$) in wild-type cells. In addition, the readily releasable vesicle pool of *Munc13-2* KO neurons was unchanged as determined by application of hypertonic sucrose solution ($0.94 \pm 0.21 \text{ nC}$, $n = 10$, for wild-type excitatory neurons vs. $0.93 \pm 0.14 \text{ nC}$, $n = 10$, for *Munc13-2* KO excitatory cells; Fig. 2C; data for inhibitory neurons not shown).

In contrast to the *Munc13-2* KO, *Munc13-1* deletion leads to a 90% reduction of readily releasable vesicles and evoked transmitter release (Fig. 2A; ref. 3). This result indicates a partial redundancy of *Munc13* isoforms in hippocampal neurons. To circumvent this redundancy, we generated *Munc13-1/2* DKO mice by interbreeding homozygous *Munc13-2* KOs and heterozygous *Munc13-1* KOs (3). Homozygous *Munc13-2* KOs from the same litters, which are indistinguishable from wild-type (see above), served as control in all subsequent analyses. Homozygous *Munc13-1/2* DKOs (E18) expressed neither *Munc13-1* nor *Munc13-2* (Figs. 1D and 3), were very fragile, and often were born dead. All DKOs that were born alive died within 1 h after birth. However, the brain and spinal cord from DKO mice (E18) showed normal cell density and cytoarchitecture (Fig. 4A and B), and the expression levels of all tested synaptic and nonsynaptic proteins (*Munc13-3*, *Munc18-1*, RIM, Rab3A,

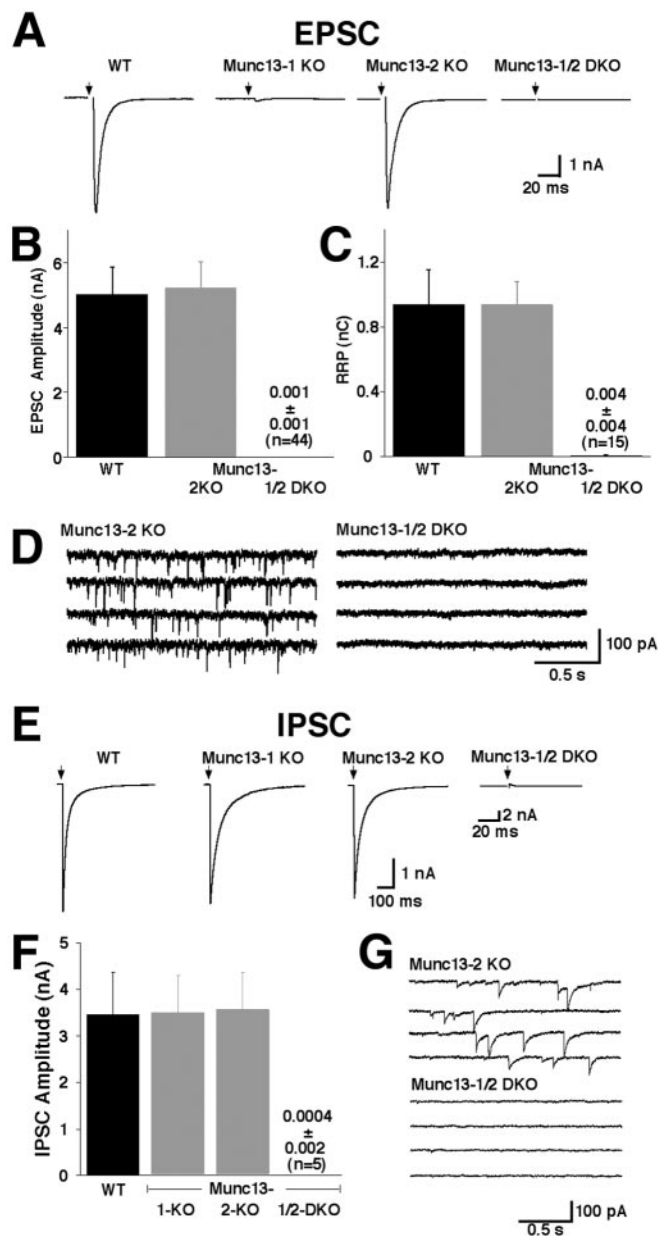


Fig. 2. Complex functional redundancy of Munc13 isoforms. (A) Examples of EPSCs recorded from cells of the indicated genotypes. (B) Mean EPSC amplitudes measured in cells of the indicated genotypes. (C) Mean readily releasable vesicle pool sizes in cells of the indicated genotypes as estimated by the charge integral measured after release induced by application of 500 mOsm hypertonic sucrose solution for 4 s. (D) mEPSC activity recorded in cells of the indicated genotypes. Holding potential -70 mV. (E) Examples of IPSCs recorded from cells of the indicated genotypes. Munc13-1/2 DKO inhibitory neurons were identified after each experiment by detection of mIPSC events induced by application of α -latrotoxin. (F) Mean IPSC amplitudes measured in cells of the indicated genotypes. (G) mIPSC activity recorded in cells of the indicated genotypes. Pipette solution contained 140 mM KCl.

SNAP25, syntaxin 1A, synaptobrevin 2, complexin 1/2, and tubulin) in Munc13-1/2 DKO brains were very similar to those of wild-type animals (Fig. 3). Detection of subtle changes in protein expression will require larger numbers of DKO mice, which could not be generated so far.

Because of the perinatal lethality of the Munc13-1/2 DKOs, we used primary hippocampal neurons from embryonic (E18) Munc13-1/2 DKO and Munc13-2 KO littermates for functional

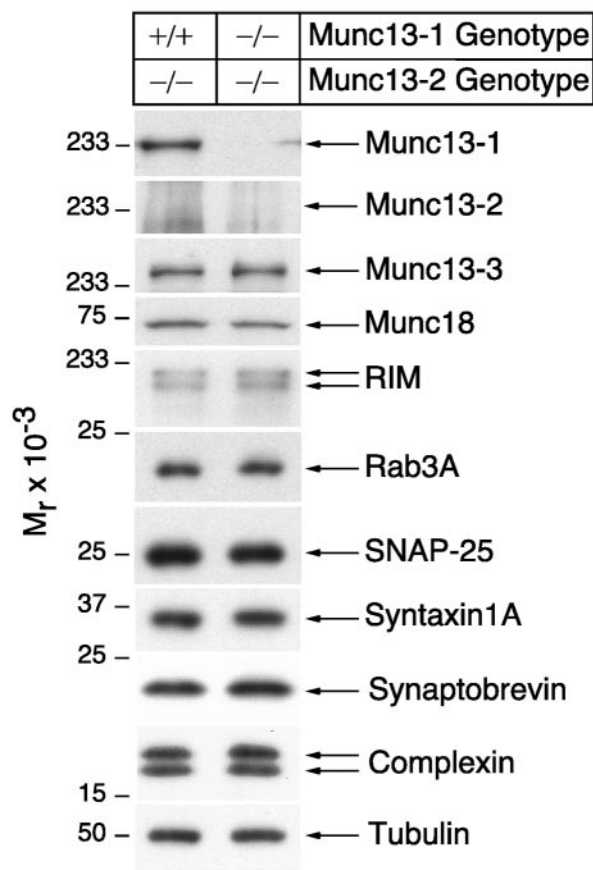


Fig. 3. Normal expression of synaptic proteins in Munc13-1/2 DKO brains. Brain homogenates of the indicated genotypes were analyzed by Western blotting using specific antibodies to the indicated proteins.

analyses. Munc13-1/2 DKO neurons developed a normal cell morphology in culture (Fig. 4C). Whole cell recordings from these neurons showed normal voltage-dependent Na^+ , K^+ , and Ca^{2+} currents (not shown). However, of a total of 45 recorded Munc13-1/2 DKO neurons, none showed any sign of evoked or spontaneous release at all times tested (8–15 DIV; Fig. 2), and all recorded neurons were insensitive to application of hypertonic sucrose solution (Fig. 2C), indicating a complete absence of release-competent vesicles. Assuming that no deficit in synaptogenesis contributes to the Munc13-1/2 DKO phenotype (see below), these data lead to three important conclusions: (i) Because release by hypertonic shock does not require Ca^{2+} channel activity (15), the complete absence of spontaneous, hypertonically induced, or evoked release in Munc13-1/2 DKO cells indicates a complete loss of fusion competent vesicles. (ii) Because all modes of vesicular release (spontaneous, action potential evoked, and hypertonically evoked) are equally abolished in Munc13-1/2 DKO cells, they seem to depend on the same vesicular priming process and draw from the same pool of release-competent, primed vesicles, indicating that hypertonically induced responses are a faithful measure of the pool of fusion competent vesicles. (iii) No Munc13-independent vesicle-priming pathways exist in mature hippocampal neurons in culture. We know that inhibitory cells were equally affected by the Munc13-1/2 DKO because strong stimulation of release by α -latrotoxin at the end of each experiment allowed the successful induction of very rare mPSC events (see below) and, thus, identification of transmitter phenotypes on the basis of mPSC shape, amplitude, and pharmacology. Using this approach, 5 of the 45 recorded cells were shown to be GABAergic.

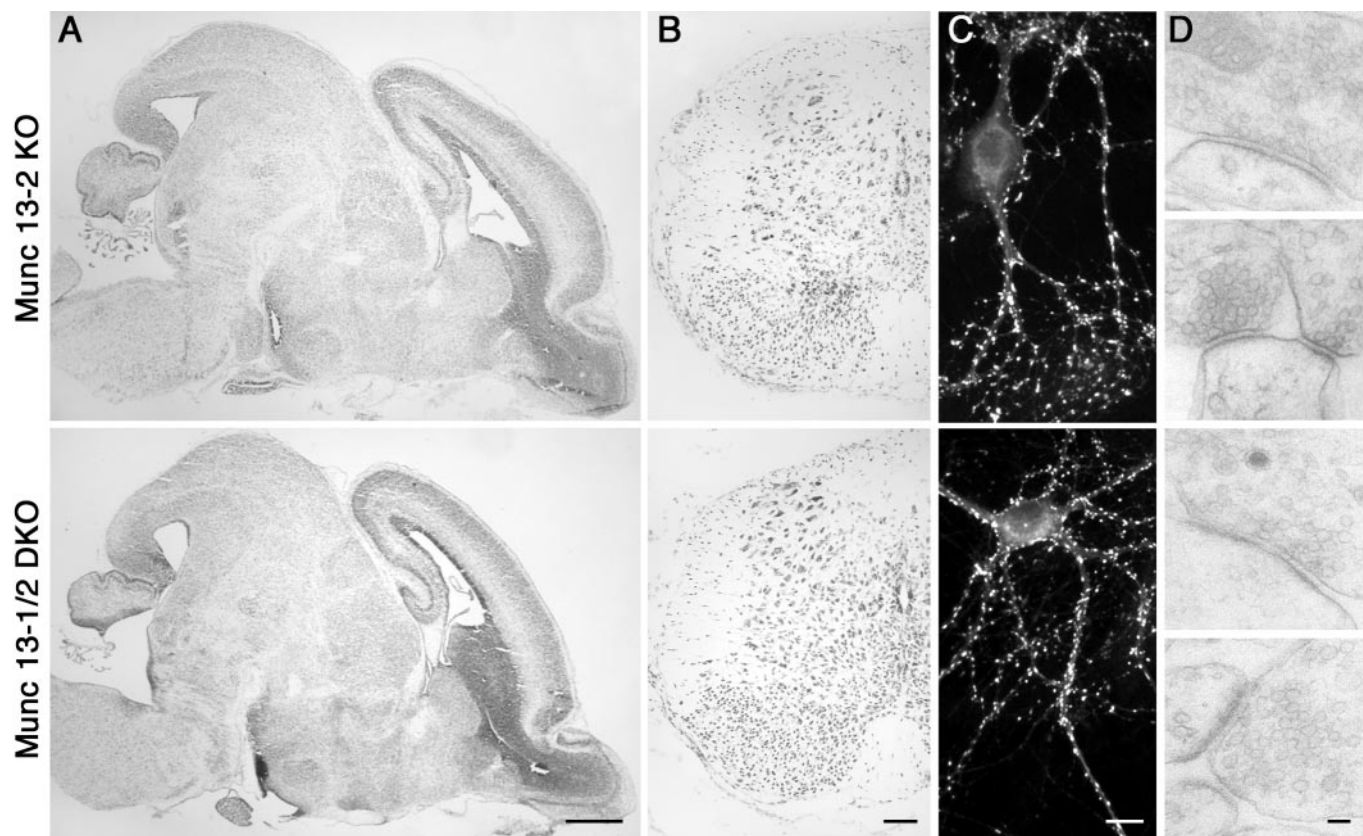


Fig. 4. Normal morphology of Munc13-1/2 DKO brains and cultured cells. (A) Nissl-stained sagittal section of brains from E18 mice of the indicated genotype. (Bar = 500 μm .) (B) Nissl-stained coronal sections of spinal cord from E18 mice of the indicated genotype. (Bar = 100 μm .) (C) Cultured hippocampal neurons from E18 mice of the indicated genotype (12 DIV) stained for the synapse specific marker synaptophysin. (Bar = 10 μm .) (D) Electron micrographs of synapses of the indicated genotypes. (Bar = 100 nm.)

To test whether postsynaptic development is impaired in Munc13-1/2 DKO cells, we used the spider toxin α -latrotoxin, which was shown to partially circumvent the need for Munc13-1 in vesicular release (3). We found that application of 1 nM α -latrotoxin induced mEPSC and mIPSC activity in Munc13-1/2 DKO neurons, but the release rate was much lower than that of wild-type-like Munc13-2 KO control cells (Fig. 5 A–D). Five minutes after a 60-s application of 1 nM α -latrotoxin, Munc13-2 KO control neurons exhibited mEPSCs at a frequency of 23.4 ± 3.9 Hz ($n = 17$; Fig. 5 A and B). The average amplitude of mEPSCs was 22.7 ± 2.4 pA (Fig. 5B). Both mEPSC amplitude and frequency after α -latrotoxin treatment are similar to wild-type values (not shown). In contrast, Munc13-1/2 DKO neurons showed mEPSC-like events after α -latrotoxin treatment at a frequency of only 0.074 ± 0.024 Hz ($n = 17$; Fig. 5 A and B). However, the amplitude of these rare mEPSC events was similar to that observed in wild-type (3, 11) and Munc13-2 KO neurons (25.6 ± 2.6 pA, $n = 17$; Fig. 5B). mIPSC-like events in the presence of α -latrotoxin were observed in five Munc13-1/2 DKO cells at low frequency (0.14 ± 0.07 Hz, $n = 5$ vs. 15 ± 5 Hz, $n = 4$, in Munc13-2 KO cells) but with amplitudes (63 ± 14 pA, $n = 5$) comparable to wild-type-like Munc13-2 KO values (45.5 ± 6.3 pA, $n = 4$; Fig. 5 C and D). These data and the fact that detected mPSCs were blocked by the appropriate antagonists (Fig. 5 A and C) indicate that postsynaptic equipment with and accumulation of functional α -amino-3-hydroxy-5-methyl-4-isoxazolepropionic acid (AMPA) or GABA receptors is not impaired. Indeed, the localization of the glutamate receptor subunit GluR2 in Munc13-1/2 DKO neurons was indistinguishable from control data at the light microscopic level and concentrated in areas facing synaptophysin-positive presynaptic terminals (not shown). More-

over, the overall cell surface density of receptors was normal in Munc13-1/2 DKO neurons as determined by the responses of DKO and control cells to 10 μM kainate or 1 μM GABA (Fig. 5E).

Density and Ultrastructure of Synapses in Munc13-1/2 DKO Neurons. We next examined synapse density and ultrastructure in cultures from Munc13-1/2 DKO and Munc13-2 KO control hippocampi. The total number of synaptophysin-positive synapses per cell (not shown) and the density of synapses per μm^2 of MAP-2-positive dendrites were very similar in Munc13-2 KO control (0.23 ± 0.04 per μm^2 , $n = 9$ cells) and Munc13-1/2 DKO neurons (0.29 ± 0.02 per μm^2 , $n = 10$ cells) (Fig. 4C). Thus, synapse formation in culture as determined by light microscopic criteria is not altered on complete shut down of transmitter release in Munc13-1/2 DKO neurons.

To detect effects of the loss of Munc13 priming factors or lack of synaptic activity on synapse assembly, we analyzed the ultrastructure of Munc13-1/2 DKO synapses. We observed typical synaptic structures in Munc13-1/2 DKO neurons (Fig. 4D). In particular, we found similar numbers of docked vesicles per synapse in Munc13-2 KO (2.7 ± 0.3 , $n = 56$ synapses) and Munc13-1/2 DKO cells (2.1 ± 0.2 , $n = 62$ synapses). The length of active zones was larger in Munc13-1/2 DKO synapses (380 ± 27 nm, $n = 62$) than in Munc13-2 KO control synapses (263 ± 19 nm, $n = 56$; $P < 0.05$). As a consequence, the number of docked vesicles per μm active zone was lower in Munc13-1/2 DKO synapses (5.9 ± 0.8 per μm , $n = 62$) than in Munc13-2 KO control synapses (9.2 ± 0.8 , $n = 56$; $P < 0.05$). Because of the considerable variability of synaptic ultrastructure in culture, these data have to be interpreted cautiously. Nevertheless, they

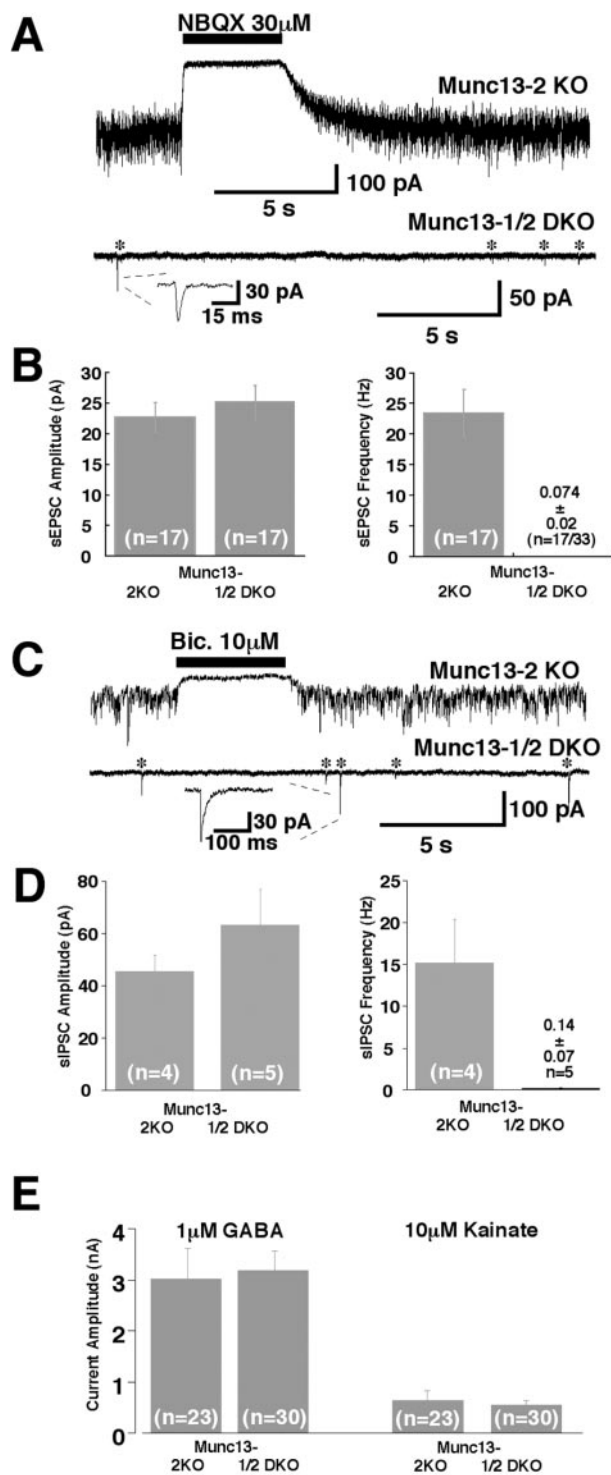


Fig. 5. Normal postsynaptic responsiveness in release-incompetent Munc 13-1/2 double-deficient neurons. (A) Examples of mEPSC activity in cells of the indicated genotypes after application of 1 nM α -latrotoxin for 1 min. Note that signals are blocked by 2,3-dihydroxy-6-nitro-7-sulfamoylbenzo[*f*]quinoxaline (NBQX). Stars indicate mEPSC events. (Inset) Individual mEPSC (expanded scale). (B) Average mEPSC amplitude and frequency in cells of the indicated genotypes after treatment with 1 nM α -latrotoxin. (C) Examples of mIPSC activity in cells of the indicated genotypes after application of 1 nM α -latrotoxin for 1 min. Note that signals are blocked by bicuculline. Stars indicate mIPSC events. Inset shows individual mIPSC (expanded scale). (D) Average mIPSC amplitude and frequency in cells of the indicated genotypes after treatment with 1 nM α -latrotoxin. (E) Mean peak current responses evoked by exogenous application of GABA and kainate recorded from cells of the indicated genotypes.

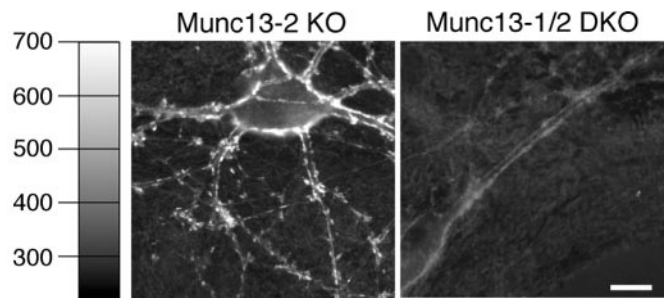


Fig. 6. No endocytosis in release-incompetent Munc13-1/2 DKO neurons. Localization of endocytotically active synapses by activity-dependent FM1-43 staining in cells of the indicated genotypes. Images show cells after staining and wash. (Bar = 10 μ m.)

indicate that the striking phenotype of Munc13-1/2 DKO neurons is not caused by a major dysfunction in synapse assembly, and synapses assemble almost normally even in the complete absence of spontaneous and evoked transmitter release.

Endocytosis in Munc13-1/2 DKO Neurons. To test whether the lack of Munc13 priming factors and the resulting complete block of synaptic release affect endocytosis, we assayed stimulation-induced uptake of FM1-43 with quantitative fluorescence microscopy as a measure of synaptic endocytosis in cultured neurons (6, 16–18). Munc13-2 KO neurons showed normal FM1-43 staining/endocytosis (Fig. 6 *Left*). In contrast, Munc13-1/2 DKO synapses were never stained in the presence of FM1-43 (Fig. 6 *Right*), indicating that DKO cells not only are unable to exocytose but also lack Ca^{2+} -triggered endocytotic activity. Assuming that Munc13s are not directly involved in endocytosis, a notion that is supported by the rather normal ultrastructural characteristics of Munc13-1/2 DKO synapses, these data indicate that synaptic endocytosis is coupled to exocytosis and does not take place when exocytosis is arrested.

Rescue of Munc13-1/2 DKO Synapses by Overexpression of Munc13-1 or Munc13-2. We next assayed the consequences of Semliki Forest virus-mediated overexpression of Munc13-1 or Munc13-2 isoforms in Munc13-1/2 DKO neurons (9). Irrespective of the Munc13 isoform used for overexpression, we obtained almost complete rescue of synaptic amplitudes to wild-type like control levels (i.e., levels measured in Munc13-2 KO littermates). EPSC amplitudes of Munc13-2 KO neurons were 1.3 ± 0.3 nA ($n = 17$), whereas Munc13-1/2 DKO neurons overexpressing either Munc13-1 or Munc13-2 showed EPSC amplitudes of 0.84 ± 0.14 nA ($n = 25$) and 0.78 ± 0.11 nA ($n = 32$), respectively. Similar rescue efficiencies were observed in inhibitory neurons. These data show that the absence of Munc13 priming proteins is the sole reason for the complete inability of double mutant synapses to release transmitter. The fact that rescued EPSC amplitudes approach wild-type levels irrespective of the overexpressed Munc13 isoform suggests that all preformed synapses accept both Munc13 isoforms as a priming factor. This result is remarkable because, in wild-type neurons, 90% of all glutamatergic synapses are exclusively dependent on Munc13-1 and do not contain Munc13-2 (3).

Discussion

Munc13-1 deletion mutant neurons are characterized by a dramatic reduction in readily releasable vesicle pools and evoked transmitter secretion. Interestingly, this phenotype is specific for glutamatergic neurons whereas GABAergic cells are completely unaffected. Within a given Munc13-1-deficient glutamatergic neuron, a large fraction of synapses is completely shut down

whereas the remaining synapses release with normal probability (3, 6). In contrast to Munc13-1, deletion of Munc13-3, the only Munc13 isoform that is coexpressed with Munc13-1 in cerebellum, has very mild phenotypic consequences that are not compatible with an essential role of Munc13-3 in GABAergic synaptic vesicle priming (10). The present paper shows that the same is true for Munc13-2 (Fig. 2).

The surprising lack of phenotypic alterations in Munc13-2 and Munc13-3 KO has led us to speculate that the specificity of Munc13-1-mediated vesicle priming for glutamatergic synapses is due to the fact that GABAergic neurons use a Munc13-independent priming mechanism (3). We show now that this is not the case in hippocampal neurons where the only two Munc13 isoforms present, Munc13-1 and Munc13-2, exhibit a complex pattern of redundancy. In GABAergic hippocampal neurons, the loss of Munc13-1 or Munc13-2 can be compensated for by the presence of the respective other (Fig. 2 E and F) whereas, in glutamatergic hippocampal neurons, Munc13-1 can compensate for Munc13-2 loss but not vice versa (Fig. 2). In both cell types, the complete absence of Munc13 priming factors leads to elimination of readily releasable vesicles and total arrest of synaptic vesicle priming (Fig. 2), demonstrating that Munc13-mediated vesicle priming is a common and essential feature of two different fast neurotransmitter systems and that no Munc13-independent vesicle priming mechanisms exist in these mature cells. Interestingly, recent data from adrenal chromaffin cells suggest that Munc13s may also be involved in the priming of catecholamine-containing chromaffin granules (19). Moreover, release of acetylcholine and GABA in *C. elegans* is absolutely dependent on the Munc13 homologue Unc-13 (5). We therefore propose that Munc13-mediated vesicle priming is an essential component of all fast neurotransmitter systems.

As mentioned above, most synapses in excitatory Munc13-1 KO neurons are completely shut down whereas a small subpopulation functions normally (3, 6). The fact that synaptic release activity in Munc13-1-deficient neurons is completely abolished when Munc13-2 is also deleted (Fig. 2) suggests that active synapses in Munc13-1 KO neurons are exclusively driven by Munc13-2. Thus, glutamatergic cells form two types of synapses that are differentially equipped with Munc13-1 and Munc13-2. In contrast, Munc13-1 and Munc13-2 are completely redundant in GABAergic hippocampal neuron, suggesting that, in wild-type GABAergic neurons, all synapses are equipped with both Munc13-1 and Munc13-2. FM1-43 imaging experiments (6) showed that the distribution of Munc13-1-independent synapses does not follow a particular somatic or dendritic localization pattern. Although it is possible that the culture conditions conceal such morphological patterns, we suggest that the heterogeneity of synapses is intrinsically present. Our view

is supported by data from *in situ* hybridization experiments and semiquantitative immunoelectron microscopy studies showing that only a subpopulation of type I presynaptic compartments formed by Munc13-1-expressing cells contain Munc13-1 (20). Thus, glutamatergic neurons *in situ* likely express a similarly heterogeneous synapse population with respect to Munc13 isoform content and dependence. That individual axons *in situ* can indeed form functionally different types of synapses is evident from experiments in cortical (21, 22) and hippocampal (23) slices.

A particularly interesting conclusion from the present study is that, even in the permanent and complete absence of spontaneous and evoked transmitter release in most areas of the central nervous system (compensation by Munc13-3 is likely to occur only in the cerebellum; ref. 10), brain and spinal cord develop normally (Fig. 4 A and B). Moreover, release-incompetent synapses in cultured hippocampal Munc13-1/2 DKO neurons are formed and maintained at normal densities (Fig. 4C) and have normal postsynaptic sensitivity characteristics (Fig. 5). Finally, inactive Munc13-1/2 DKO synapses in culture have an ultrastructural morphology that exhibits all classical features of mature synapses and is only slightly altered in comparison with wild-type-like control synapses (Fig. 4D). In that respect, our study extends published data on Munc18-1-deficient mice in which transmitter release is also completely shut down (24). Synapses in Munc18-1-deficient brains are formed normally during brain development but degenerate as the embryo matures. This result led to the conclusion that synaptic transmitter release is not necessary for the initial formation of synapses but essential for their maintenance (24). We found no evidence for degenerative processes in release-incompetent Munc13-1/2 double-deficient brains. In particular, spinal cord and brainstem, which more or less exclusively express Munc13-1 and Munc13-2 (8, 10), were intact (Fig. 4A). We conclude that synaptic activity is not only dispensable for initial synaptogenesis (24) but also not necessary for the basic maintenance of synapses and many of their characteristics. The degeneration observed in Munc18-1-deficient brains (24) may be due to the perturbation of a Munc18-1-dependent process that is not directly related to transmitter secretion.

We thank K. Hellmann, T. Hellmann, I. Herfort, S. Wenger, and A. Zeuch for excellent technical assistance, and F. Benseler and I. Thanhäuser for DNA sequencing and oligonucleotide synthesis. We are indebted to D. Riedel for invaluable help with electron microscopy. We are grateful to the staff of the animal facility at the Max-Planck-Institute for Experimental Medicine for blastocyst injections and maintenance of mouse colonies. This study was supported by grants from the Deutsche Forschungsgemeinschaft (SFB406/A1 to N.B. and Ro1296/5-1 to C.R.). N.B. and C.R. are Heisenberg Fellows of the Deutsche Forschungsgemeinschaft.

- Südhof, T. C. (1995) *Nature (London)* **375**, 645–653.
- Zucker, R. S. (1996) *Neuron* **17**, 1049–1055.
- Augustin, I., Rosenmund, C., Südhof, T. C. & Brose, N. (1999b) *Nature (London)* **400**, 457–461.
- Aravamudan, B., Fergestad, T., Davis, W. S., Rodesch, C. K. & Broadie, K. (1999) *Nat. Neurosci.* **2**, 965–971.
- Richmond, J. E., Davis, W. S. & Jorgensen, E. M. (1999) *Nat. Neurosci.* **2**, 959–964.
- Rosenmund, C., Sigler, A., Augustin, I., Reim, K., Brose, N. & Rhee, J.-S. (2002) *Neuron* **33**, 411–424.
- Brose, N., Hofmann, K., Hata, Y. & Südhof, T. C. (1995) *J. Biol. Chem.* **270**, 25273–25280.
- Augustin, I., Betz, A., Herrmann, C., Jo, T. & Brose, N. (1999a) *Biochem. J.* **337**, 363–371.
- Betz, A., Thakur, P., Junge, H. J., Ashery, U., Rhee, J. S., Scheuss, V., Rosenmund, C., Rettig, J. & Brose, N. (2001) *Neuron* **30**, 183–196.
- Augustin, I., Korte, S., Rickmann, M., Kretschmar, H. A., Südhof, T. C., Herms, J. W. & Brose, N. (2001) *J. Neurosci.* **21**, 10–17.
- Reim, K., Mansour, M., Varoqueaux, F., McMahon, H. T., Südhof, T. C., Brose, N. & Rosenmund, C. (2001) *Cell* **104**, 71–81.
- Thomas, K. R. & Capecchi, M. R. (1987) *Cell* **51**, 503–512.
- Bekkers, J. M. & Stevens, C. F. (1991) *Proc. Natl. Acad. Sci. USA* **88**, 7834–7838.
- Rosenmund, C., Feltz, A. & Westbrook, G. L. (1995) *J. Neurosci.* **15**, 2788–2795.
- Rosenmund, C. & Stevens, C. F. (1996) *Neuron* **16**, 1197–1207.
- Ryan, T. A., Smith, S. J. & Reuter, H. (1996) *Proc. Natl. Acad. Sci. USA* **93**, 5567–5571.
- Murthy, V. N., Sejnowski, T. J. & Stevens, C. F. (1997) *Neuron* **18**, 599–612.
- Cochilla, A. J., Angleson, J. K. & Betz, W. J. (1999) *Annu. Rev. Neurosci.* **22**, 1–10.
- Ashery, U., Varoqueaux, F., Voets, T., Betz, A., Thakur, P., Koch, H., Neher, E., Brose, N. & Rettig, J. (2000) *EMBO J.* **19**, 3586–3595.
- Betz, A., Ashery, U., Rickmann, M., Augustin, I., Neher, E., Südhof, T. C., Rettig, J. & Brose, N. (1998) *Neuron* **21**, 123–136.
- Reyes, A., Lujan, R., Rozov, A., Burnashev, N., Somogyi, P. & Sakmann, B. (1998) *Nat. Neurosci.* **1**, 279–285.
- Thomson, A. M. (1997) *J. Physiol.* **502**, 131–147.
- Scanziani, M., Gähwiler, B. H. & Chrapak, S. (1998) *Proc. Natl. Acad. Sci. USA* **95**, 12004–12009.
- Verhage, M., Maia, A. S. Plomp, J. J., Brussaard, A. B., Heeroma, J. H., Vermeer, H., Toonen, R. F., Hammer, R. E., van den Berg, T. K., Missler, M., Geuze, H. J. & Südhof, T. C. (2000) *Science* **287**, 864–869.